Palaeogeography, Palaeoclimatology, Palaeoecology 385 (2013) 95–105

Contents lists available at SciVerse ScienceDirect

Palaeogeography, Palaeoclimatology, Palaeoecology

journal homepage: www.elsevier.com/locate/palaeo

Paleoatmospheric pCO_2 fluctuations across the Cretaceous–Tertiary boundary recorded from paleosol carbonates in NE China

Chengmin Huang [a,*], Gregory J. Retallack [b], Chengshan Wang [c], Qinghua Huang [d]

[a] Department of Environmental Science and Engineering, Sichuan University, Chengdu, Sichuan 610065, China
[b] Department of Geological Sciences, University of Oregon, Eugene, OR 97403, USA
[c] School of Earth Science and Resources, China University of Geosciences, Beijing 100083, China
[d] Exploration and Development Research Institute, Daqing Oilfield Company Ltd., Daqing, Helongjiang 163712, China

ARTICLE INFO

Article history:
Received 7 October 2011
Received in revised form 2 December 2012
Accepted 1 January 2013
Available online 18 January 2013

Keywords:
Cretaceous
Tertiary
Atmospheric CO_2
Paleosol
Pedogenic carbonate
Deccan Traps
Chicxulub impact
China

ABSTRACT

A dramatic change in atmospheric composition has been postulated because of global carbon cycle disruption during the Cretaceous (K)–Tertiary (T) transition following the Chicxulub impact and Deccan Trap eruptions. Here, pedogenic carbonates were collected from drill core of a borehole (SK-1 (N)) straddling the Late Cretaceous and early Paleocene strata in the Songliao Basin, northeast China, to reconstruct atmospheric CO_2 concentrations using a paleosol paleobarometer. Our estimates for atmospheric pCO_2 from paleosol carbonates range between 277 ± 115 ppmv and 837 ± 164 ppmv between 67.8 Ma and 63.1 Ma. One large (~66–65.5 Ma) and several small CO_2 spikes (~64.7–~64.2 Ma) during the latest Maastrichtian to earliest Danian are reported here and incorporated with previously published pCO_2 estimates also estimated from paleosol carbonates. These CO_2 spikes are attributed to one-million-year-long emplacement of the large Deccan flood basalts along with the extraterrestrial impact at the K–T boundary.

1. Introduction

The K–T boundary was marked by one of the largest mass extinctions during the past 500 million years (Peters, 2008), and several hypotheses have been proposed to explain the mass extinction at the K–T boundary. The impact hypothesis was introduced to account for the mass extinction (Alvarez et al., 1980), and increasing numbers of scientists attribute the mass extinction to the Chicxulub impact event (Hildebrand et al., 1991; Kring, 2007; MacLeod et al., 2007; Miller et al., 2010; Schulte et al., 2010). Global environmental consequences of the impact included release of large quantities of water, dust, and climate-forcing sulfuric and nitric acidic gases (Retallack, 1996), extensive combustion of biomass or fossil organic matter (Wolbach et al., 1988; Melosh et al., 1990; Ivany and Salawitch, 1993; Jones and Lim, 2000; Belcher et al., 2009), and mega-tsunami and ejecta debris deposition (Claeys et al., 2002). Alternatively, a continental flood basalt hypothesis has also been used to explain the K–T mass extinction pattern, due to abrupt global cooling resulting from the voluminous release of sulfur dioxide and dust into the atmosphere for single eruptive events in the Deccan flood basalt traps (Keller et al., 2008; Chenet et al., 2009; Courtillot and Fluteau, 2010), or to later greenhouse warming with increase of atmospheric CO_2 once dust, soot and aerosols fell to the ground (Duncan and Pyle, 1988; O'Keefe and Ahrens, 1989; Crowley and Berner, 2001). In addition, multicausal models including impact, volcanic activity, marine regression, and changes in global and regional climatic patterns have been linked to the extinction event (Keller, 2001; Keller et al., 2003, 2009; MacLeod, 2003; Archibald et al., 2010; Keller et al., 2010).

A significant perturbation of the global carbon cycle has been predicted from extinctions themselves, as well as from impact and volcanic eruption near the K–T boundary. It was hypothesized that atmospheric CO_2 would rise dramatically across the K–T transition due to massive amounts of CO_2 from Chicxulub's target carbonate-rich lithologies and the projectile (O'Keefe and Ahrens, 1989; Agrinier et al., 2001; Kring, 2007), from widespread large wildfires (Melosh et al., 1990; Wolbach et al., 1990; Ivany and Salawitch, 1993; Durda and Kring, 2004), from intruded or impacted coal or hydrocarbons (Belcher et al., 2005; Harvey et al., 2008; Belcher et al., 2009), from reduction in worldwide marine primary productivity (D'Hondt et al., 1998; Aberhan et al., 2007; Maruoka et al., 2007), and from degassing of mantle volatiles during several short eruptions of the Deccan Traps (Courtillot et al., 1986; Officer et al., 1987; Self et al., 2006; Kring, 2007; Chenet et al., 2009).

Estimated atmospheric CO_2 concentrations across the K–T transition are tests of these hypotheses. An abrupt pCO_2 fluctuation at the K–T boundary has been examined using both stomatal index of fossil plants (Beerling et al., 2002; Retallack, 2009a) and a paleosol barometer (Nordt et al., 2002, 2003). However, disparity between magnitude and

* Corresponding author.
E-mail address: cmhuangscu@gmail.com (C. Huang).

0031-0182/$ – see front matter © 2013 Elsevier B.V. All rights reserved.
http://dx.doi.org/10.1016/j.palaeo.2013.01.005

duration of CO_2 concentration in these studies highlights the need for more records with greater precision and temporal resolution (Arens and Jahren, 2002; Retallack, 2004). In the past, lack of information about key parameters such as soil respiration for the pedogenic CO_2 paleobarometer of Cerling (1991) have limited their precision in determining ancient CO_2 levels, but now a variety of proxies for soil respiration are available (Retallack, 2009b; Breecker et al., 2010; Royer, 2010; Cotton and Sheldon, 2012).

The Songliao Basin of China has thick sequences of Jurassic–Paleogene terrestrial strata (Wan et al., 2007), including carbonate-nodule-bearing paleosols suitable for determination of paleoatmospheric CO_2 (Huang et al., 2010). Our study uses selected carbonate paleosols in northeast China in order to: (1) estimate atmospheric pCO_2 levels across the K–T boundary using a paleosol CO_2 paleobarometer and supplement the global database of CO_2 concentrations; and (2) indicate the source(s) for the change in pCO_2, if any.

2. Geological setting

Within one of the largest Cretaceous landmasses (Scotese et al., 1988), the Songliao Basin in northeast China covers an area of ~260,000 km^2 (Fig. 1). The basin is filled predominantly with volcaniclastic, alluvial fan, fluvial, and lacustrine sediments of Late Jurassic, Cretaceous, and Paleogene ages on a pre-Mesozoic basement (Wang et al., 2009). Mesozoic and Cenozoic terrestrial strata are up to 7000 m thick above the basement unconformity (Gao et al., 1994; Wu et al., 2009).

A scientific borehole (SK-1 (N)) was drilled in 2007 that covered the complete Upper Cretaceous to Paleocene section in the basin in a total depth of 1541.66 m. The Upper Mingshui Formation of latest Cretaceous and earliest Paleogene (Maastrichtian–Paleocene) ages is composed of variegated sandstone and gray-green mudstone intercalated with brown mudstone (Wang et al., 2008).

Although lacking a diagnostic boundary claystone, iridium anomaly, glass spherules and shocked minerals, the K–T boundary is recognizable palynologically (Chen et al., 2004; Kring, 2007; Therrien et al., 2007), by extinction of some key taxa, e.g., aquilapollens (Nichols, 1990; Braman and Sweet, 1999; Sweet and Braman, 2001; Chen et al., 2004; Liu et al., 2009). Here, the K–T boundary in the Songliao Basin from the Drill SK-1 (N) was interpolated at depth of 360.6 m (±10 m) below the surface, because 51 species of spores, gymnosperm pollen, angiosperm pollen (*Normapolles* and *Aquilapolles*) disappeared above this depth, in contrast with the strata below the depth (Li et al., 2011). This is supported from the Baitoushan section, in the Jiayon Bain, also located in Helongjiang, NE China, where the base of coal-bearing Wuyun Formation and the top of the Furao Formation coincide with nonmarine K–T boundary based on biostratigraphic analysis (Chen et al., 2004; Liu et al., 2009). About 10 species of *Aquilapolles* are observed to indicate late Maastrichtian age of Furao Formation (Chen et al., 2004), and a SHRIMP U–Pb zircon age of rhyolitic crystal tuff, ~9.3 m below the top of the Furao Formation strata is 66 ± 1 Ma, only 0.5 Ma older than the recommended K–T boundary age in the International Stratigraphic Chart (Li et al., 2004). However, the K–T boundary should be close to the depth of 360.6 m given that paucity of pollen and spores within approximate 100 m of section within 360.6 m to 263.4 m (Li et al., 2011; Deng et al., 2013). The geomagnetic polarity timescale for the borehole (SK-1 (N)) was determined by combining magnetostratigraphy, SIMS U–Pb zircon geochronology and lithostratigraphy, and the top of chron 30n in the GPTS (Cande and Kent, 1995) was put at the depth of 342.1 m (Deng et al., 2013). Accordingly, the K–T boundary is estimated at ~340 m in depth of this borehole in NE China.

3. Methods

3.1. Sample collection and analytical methods

Paleosol carbonate samples were collected from 23 paleosol Bk horizons within the Upper Mingshui Formation (late Maastrichtian–early Paleocene) in the Drill SK-1 (N) at depths between 267.6 m and 480.4 m below the surface (Fig. 2). On a basis of the age of 65.58 Ma for the deposition at the depth of 342.1 m (Deng et al., 2013), the age of the paleosol horizons (*A*, Ma) for this section were extrapolated from sediment accumulation rate and the depth of the paleosol horizons (*D*, m) while the sedimentation accumulation rate (*S*, m/Ma) for the Upper Mingshui Formation was assumed as 30 m/Ma, 60 m/Ma respectively at the depth of less than 342.1 m, between 342.1 m and 530.78 m in combination with paleomagnetic analysis (Deng et al., 2013) (Eq. (1)).

$$A = 65.58 + \frac{D - 342.1}{S}. \quad (1)$$

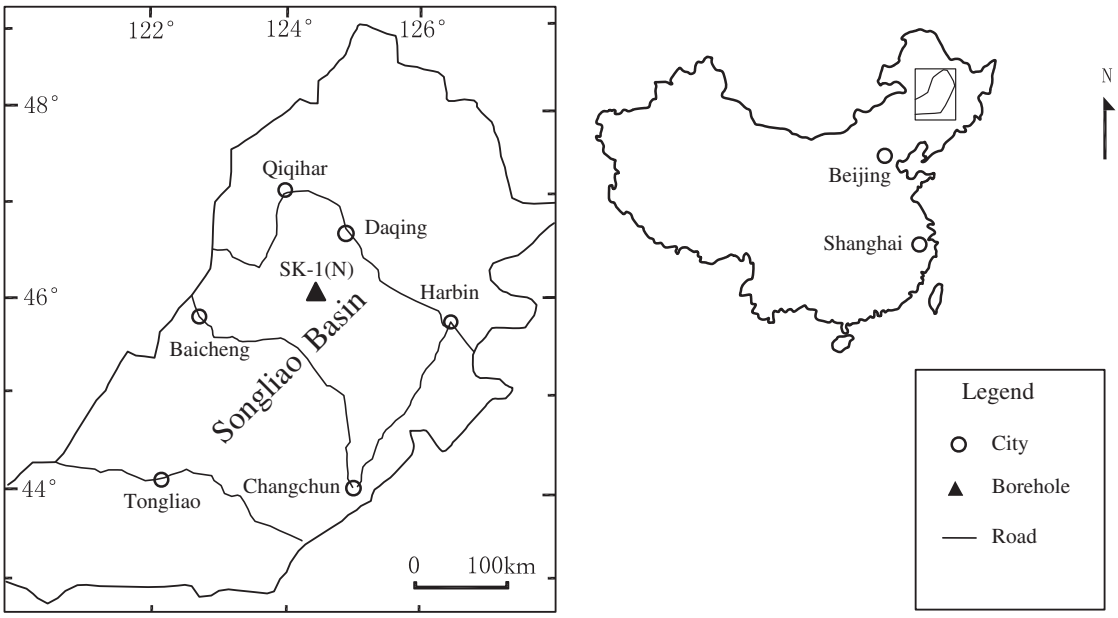

Fig. 1. Geographical position of the SK-1 (N) borehole in the Songliao Basin, northeast China.

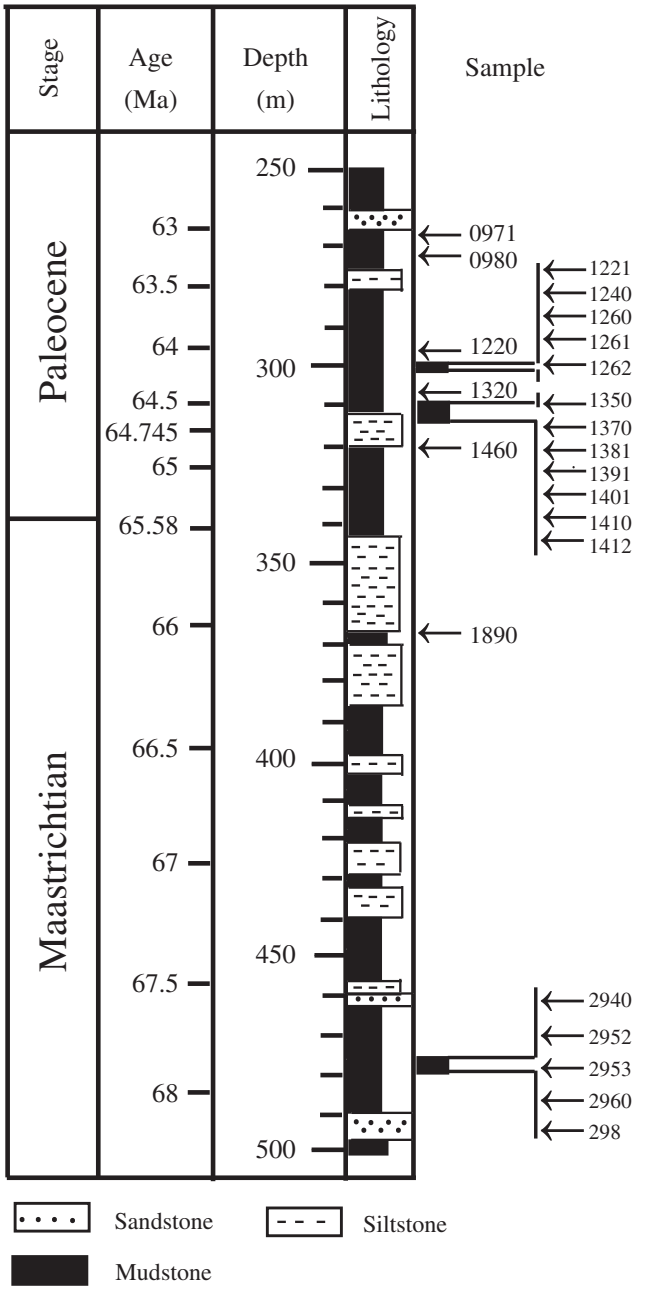

Fig. 2. Lithostratigraphic columnar section and sample horizons of the Mingshui Formation across the K–T boundary from the SK-1 (N) borehole in the Songliao Basin, northeast China.

Three samples of pedogenic carbonate nodules from each Bk horizon were sampled for stable carbon and oxygen isotopic compositions of pedogenic carbonates. ~5 mg of the micritic carbonate was sampled. These samples were reacted in vacuum with 100% phosphoric acid for at least 4 h at 25 °C, and the resulting CO_2 analyzed for carbon and oxygen isotopes with a Finnigan MAT 253 mass spectrometer at State Key Laboratory of Lithospheric Evolution, Institute of Geology and Geophysics, Chinese Academy of Sciences. The three isotopic values of separated pedogenic nodules for each Bk horizon were averaged to determine intranodule variability. The results are expressed in the notation δ‰ (per mil) relative to Peedee belemnite (PDB). Reproducibility of both $\delta^{18}O$ and $\delta^{13}C$ on standards and unknowns is within ±0.2‰.

3.2. Assumptions for atmospheric CO_2 estimation

The pedogenic carbonate CO_2 paleobarometer was used for estimates of atmospheric CO_2 concentrations (Cerling, 1999; Ekart et al., 1999):

$$P_a = P_r \cdot \frac{\left(\delta^{13}C_s - 1.0044\delta^{13}C_r - 4.4\right)}{\left(\delta^{13}C_a - \delta^{13}C_s\right)} \quad (2)$$

where P_a is atmospheric CO_2 (ppmv), P_r is soil-respired CO_2 concentration (ppmv) and $\delta^{13}C_s$, $\delta^{13}C_r$ and $\delta^{13}C_a$ are the stable carbon isotopic compositions of soil CO_2, soil-respired CO_2, and atmospheric CO_2, respectively. Variables in this equation are guessed from the following analyses and transfer functions.

The isotopic compositions of respired soil CO_2 ($\delta^{13}C_r$) is approximated by the $\delta^{13}C$ of paleosol organic carbon ($\delta^{13}C_o$) (Cerling, 1991), accordingly, $\delta^{13}C_o$ can be substituted for $\delta^{13}C_r$ in the model equation (Cerling, 1999). Considering the striking fractionation of carbon isotopic composition induced by aerobic decomposition after burial of soils (Ekart et al., 1999; Wynn, 2007), in addition to low levels of paleosol organic carbon, the isotopic compositions of well-preserved fossil terrestrial plants may also be used as a proxy of $\delta^{13}C_r$ instead of $\delta^{13}C_o$ (Robinson et al., 2002; Cleveland et al., 2008a). In cases such as this, where insufficient fossil wood was found in each paleosol, an alternative protocol is to estimate the $\delta^{13}C$ of atmospheric CO_2 ($\delta^{13}C_a$) through geological time from $\delta^{13}C$ of planktic foraminifera from high resolution marine sediments (Passey et al., 2002; Nordt et al., 2003; Retallack, 2009b), and $\delta^{13}C_o$ was calculated using Eq. (3) from Arens et al. (2000).

$$\delta^{13}C_a = \frac{\delta^{13}C_o + 18.67}{1.1}. \quad (3)$$

A five-point running average of the $\delta^{13}C$ values of planktic foraminifera were selected for $\delta^{13}C_a$ estimation within 67.8 Ma and 64.9 Ma from Deep Sea Drilling Project (DSDP) core 525A from the South Atlantic (Li and Keller, 1998) and within 64.8 Ma and 63.1 Ma from DSDP 577 from the North Pacific (Shackleton and Bleil, 1985; Zachos et al., 1989; Nordt et al., 2003), and −7.9‰ was assumed as the isotopic equilibrium fractionation value between ocean and atmospheric CO_2 (Passey et al., 2002). An assumed a value of −24.0‰ for $\delta^{13}C_a$ at 66.8 Ma calculated from $\delta^{13}C$ values of planktic foraminifera of DSDP 525A is in good agreement with an average value of ~−24.2‰ (ranging from −24.18‰ to −24.35‰) of terrestrial fossil plants from Sakhalin, Russian Far East (Hasegawa et al., 2003), in the neighborhood of the Songliao Basin, northeast China. The paleomagnetic ages of strata for $\delta^{13}C_a$ estimation from DSDP 525A and DSDP 577 were estimated following Cande and Kent (1995). The $\delta^{13}C_a$ estimated from planktic foraminifera was adopted for the paleosols at the identical ages inferred from the sedimentation rates.

Two approaches have been currently used to estimate paleotemperature in paleosol formation (Dworkin et al., 2005). One approach derives from the statistical relationship between alkaline index ($N = (K_2O + Na_2O)/Al_2O_3$, as a molar ratio) to indicate the degree of soil weathering and mean annual temperature (Sheldon et al., 2002), however, this quantification is problematic for soils formed under arid and semiarid climate because N value is unaltered or may increase with the temperature due to evaporative enrichment of Na and K within this kind of soils (Pan and Huang, 2012). Here, the isotopic composition of soil CO_2 ($\delta^{13}C_s$) comes from that of pedogenic carbonate ($\delta^{13}C_c$), corrected for temperature (T in °C) dependent fractionation from Eq. (4) (Romanek et al., 1992). We use isotopic composition of oxygen in pedogenic carbonate ($\delta^{18}O_c$) relation for modern climates to estimate temperatures, despite known diagenetic effects on oxygen isotopic composition of pedogenic carbonate after burial and potential evaporative enrichment effects under arid climates (Cerling, 1984; Quade et al.,

1989; Cerling and Quade, 1993; Mack and Cole, 2005; Tabor and Montañez, 2005). These diaganetic alterations are considered minimal because of the shallow burial depth of paleosols (<0.5 km) and limited diagenetic alteration reflected by pedogenic features (Nordt et al., 2003; Dworkin et al., 2005; Prochnow et al., 2006; Huang et al., 2010). In addition, because the Eq. (5) was derived from modern pedogenic carbonates that likely experienced some degree of evaporative enrichment (e.g., Dworkin et al., 2005), it is unnecessary to assume the total absence of evaporation (Cleveland et al., 2008a).

$$\delta^{13}C_s = \frac{\delta^{13}C_c + 1000}{\frac{11.98 - 0.12 \cdot T}{1000} + 1} - 1000 \quad (4)$$

$$T = \frac{\delta^{18}O_C + 12.65}{0.49}. \quad (5)$$

Partial pressure of respired CO_2 in soil (P_r in ppmv) depends dominantly on atmospheric CO_2 and CO_2 from respiration of roots, animals and microbes. Much higher paleo-atmospheric CO_2 concentrations estimated previously from the soil carbonate CO_2 paleobarometer than those from other paleo-pCO_2 proxies, e.g., stomatal index of fossil plants, was newly attributed to overestimation of P_r (Breecker et al., 2010; Royer, 2010). However, a proposed P_r value of 2500 ppmv for all paleosols was oversimplified (Breecker et al., 2010; Royer, 2010). For the highly significant relationship between respired soil CO_2 during late growing season and depth to Bk horizon, Retallack (2009b) established a novel transfer function between P_r and depth to carbonate, and Eq. (6) might be a better solution to reconstruct the partial pressure of respired soil CO_2 (Royer, 2010). Another relationship between summer minimum soil-respired CO_2 and mean annual precipitation has been proposed for the soils containing pedogenic carbonates (Cotton and Sheldon, 2012) using a correlation of soil productivity with precipitation. This relationship was not used for the following three reasons. First, estimation of P_r, using the scheme of Cotton and Sheldon (2012) results in large P_r errors envelopes once errors of paleoprecipitation are compounded with errors in correlation of P_r and precipitation. Second, Cotton and Sheldon (2012) are mistaken in their statement that Retallack (2009a) used mean growing season P_r. Third, use of the very lowest summer P_r values by Cotton and Sheldon (2012) gives near modern concentrations (375–454 ppm) for middle Miocene pCO_2 when applied to data of Retallack (2009b), which is too low to account for observed warmer and wetter Miocene paleoclimate (Retallack, 2009a). For compaction in paleosols, D_c was corrected using Eq. (6) in modern soils (Sheldon and Retallack, 2001).

$$P_r = 66.7 D_c + 588 \quad (6)$$

$$D_c = D_p / \left[-0.62 / \left(\frac{0.38}{e^{0.17K}} - 1 \right) \right] \quad (7)$$

where D_c (in cm), D_p (in cm) and K (in km) are original depth to carbonate nodules, depth to carbonate nodules in paleosol, and burial depth, respectively.

4. Pedogenic carbonate nodules

In most calcareous paleosols, the calcic horizon (Bk horizon) was reddened by dehydration and recrystallization of iron hydroxides to hematite (Fig. 3A,B) (Retallack, 1997, 2001; Budd et al., 2002), but some paleosols are gray in color (Fig. 3C), with little difference in color between upper and lower horizons. In terms of the morphological classification of calcretes (Goudie, 1983; Quast et al., 2006), the collected calcretes mainly appeared in forms of well-rounded to sub-rounded nodular with a diameter of 0.1–3.5 cm (Fig. 3A–F).

Micrite dominates microfabric in the carbonate nodules (Fig. 4A–D), and sparry calcite is constrained to the cracks (Fig. 4B), as is characteristic of pedogenic carbonate (Budd et al., 2002; Deutz et al., 2002; Dworkin et al., 2005; Cleveland et al., 2008b). Micritic aggregates in larger nodules have circumgranular cracks cemented by microsparite (Fig. 4C), as also known from paleosols elsewhere (Kovda et al., 2003). Displacive fabrics also are apparent where splinters of matrix have rotated (Fig. 4D), and these indicate expansion due to soil formation under low confining pressure.

5. Estimation of Cretaceous atmospheric CO_2 concentrations during the late Maastrichtian and the early Danian

Calculations of pCO_2 values from paleosol carbonates from Drill SK-1 (N) in China, range between 277 ppmv and 837 ppmv from 67.8 Ma through 63.1 Ma (Table 1), and are generally lower than the estimates of the pCO_2 range from ~400 ppm (ca. 1.4 present atmospheric level (PAL)) up to ~1400 ppm (5.0 PAL) for the interval between 80 Ma and 60 Ma by geochemical and biogeochemical models (Tajika, 1999; Berner and Kothavala, 2001; Wallmann, 2001; Berner, 2006; Fletcher et al., 2008). Also our estimates are lower than previous values of pCO_2 calculated from paleosol carbonates (Ekart et al., 1999; Cojan et al., 2000; Nordt et al., 2002), largely because of assumptions by those authors of 4000–6000 ppmv of P_r. If P_r is assumed to be only 2500 ppmv as proposed by Breecker et al. (2010), their pCO_2 values decrease to within the range of our estimates (Fig. 5). Also, averaged pCO_2 concentrations for our estimation, i.e., ~460 ppmv, during the early Paleocene is comparable with 375–404 ppmv pCO_2 estimated from fossil *Ginkgo* from Helongjiang, NE China (Quan et al., 2010).

The standard errors for atmospheric CO_2 estimates, derived from the transfer functions (above-mentioned equations) and analytic error limits, calculated from the transposed equations on a base of Gaussian error propagation used by Retallack (2009b). The standard error of the soil-respired CO_2 transfer function (Eq. (5)) reaches ±893 ppmv (Retallack, 2009b), and resulted in a variation within ±75 ppmv and ±269 ppmv of the maximal errors for atmospheric CO_2 estimates. The uncertainty from paleotemperature estimates is ±5.8 °C for Eq. (4) producing a range of ±11 ppmv and ±51 ppmv atmospheric CO_2. An analytic error of ±0.3‰ of $\delta^{13}C_r$, ±0.2‰ of $\delta^{13}C_c$ and ±0.4‰ of $\delta^{13}C_a$ gives less than ±0.1 ppmv atmospheric CO_2. In general, the errors for all atmospheric CO_2 concentration estimate fluctuate between ±78 ppmv and ±271 ppmv using Gaussian quadrature (Table 1). The ultimate errors for the mean atmospheric CO_2 concentration at each age range between ±79 ppmv and ±454 ppmv.

Using the paleosol barometer a pCO_2 peak had been previously discovered at 65.5 Ma (Nordt et al., 2002) or between 65.5 and 65.0 Ma (Nordt et al., 2003). An unusually high a peak of >2300 ppmv CO_2 at ~65 Ma was calculated from stomatal index of fossil ferns (cf. *Stenochlaena*), but this plant model remains poorly understood (Beerling et al., 2002). Another high value of 1689±430 ppmv atmospheric CO_2 was determined for ~65 Ma from 563 counts of a single leaf of *Gingko*: such low numbers of leaves and counts are statistically of low reliability (Retallack, 2009a). Discounting these extreme values and combining re-calculated pCO_2 data estimated from other pedogenic carbonates (Ekart et al., 1999; Cojan et al., 2000; Nordt et al., 2002), a pCO_2 curve spanning the Maastrichtian and Danian was composed to examine atmospheric CO_2 variation (Fig. 5). A large spike (~840 ppmv) was detected at 66.0 Ma and several small spikes (~550–~600 ppmv) at 64.7, 64.5 and 64.2 Ma, respectively.

The critical issue for identifying more spikes is the temporal resolution of atmospheric pCO_2 time series. Geochemical or biogeochemical models provide pCO_2 estimates for the entire Phanerozoic at time scales of 5–10 Ma, and so reflect major trends, but not short-term excursions (Royer et al., 2001). Many dramatic fluctuations in pCO_2 concentration occurred over short-time spans during geological time

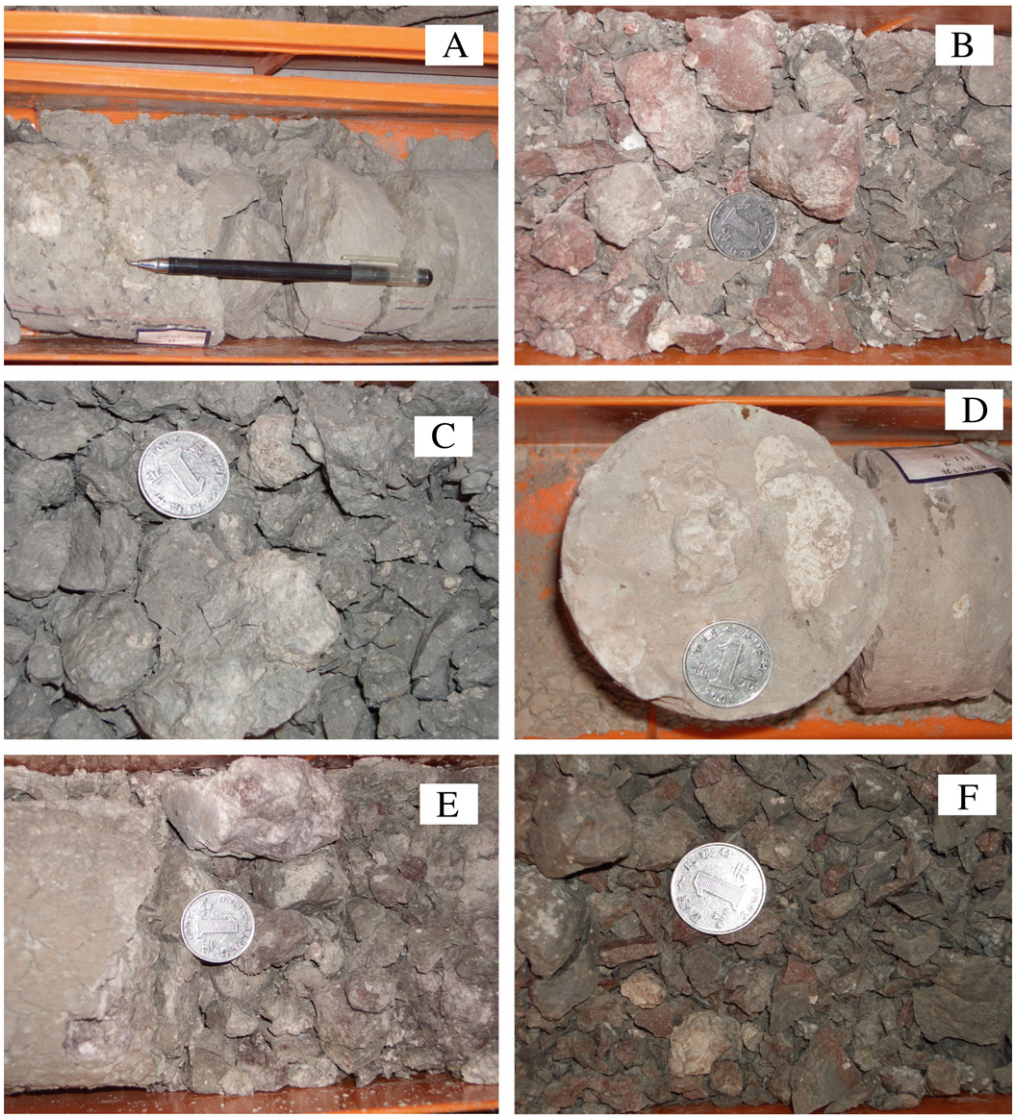

Fig. 3. Photographs of paleosols and pedogenic nodules. A) Paleosols and Bk horizon (0971), pen for scale, ~17 cm in length; B) paleosols and Bk horizon (1220), coin for scale; ~2.5 cm in diameter; C) Bk horizon and pedogenic nodules (2940), coin for scale; ~2.5 cm in diameter; D) Bk horizon and pedogenic nodules (1410), coin for scale; ~2.5 cm in diameter; and E and F) pedogenic nodules within Bk horizon (1320 and 1221, respectively), coin for scale; ~2.5 cm in diameter.

(Retallack, 2009b; Breecker et al., 2010). Atmospheric pCO_2 variations of over 100 ppmv in ~30 ka, were revealed from air trapped within ice cores, largely because of interaction between ocean and atmosphere (Fischer et al., 1999; Petit et al., 1999; Siegenthaler et al., 2005; Lourantou et al., 2010). Four atmospheric pCO_2 rises (>100 ppmv) in the duration of <100 ka have been detected since 800 ka BP to the present (Lüthi et al., 2008). In deep time, short-lived (<1 Ma) pCO_2 excursions are common, and at least 20 pCO_2 spikes have been recognized over the past 300 million years using stomatal index (Retallack, 2009a).

6. Causes for elevated atmospheric CO_2 concentrations

Low pCO_2 level during mid-Maastrichtian (68.0–67.0 Ma) ranging from 200 ppmv to 300 ppmv are compatible with evidence for a mid-Maastrichtian cool event from variation in sea level and marine $\delta^{18}O$ records (Huber et al., 2002; Miller et al., 2003).

A period of relatively high pCO_2 persisted for ~1.5 million years (66.5 Ma and 65 Ma), and the atmospheric CO_2 concentrations mostly exceeded 500 ppmv (Fig. 5). The high pCO_2 level for ~1.5 Ma is in phase with the Deccan eruptions at 67–66.5 Ma (Self et al., 2006; Chenet et al., 2007; Self et al., 2008; Jay et al., 2009). Moreover, the small CO_2 spikes within 64–65 Ma (Fig. 5) is in agreement with the third large eruption phase of the Deccan Traps (Chenet et al., 2007; Bryan et al., 2010; Hooper et al., 2010).

The peak atmospheric CO_2 level within ~66.0–~65.5 Ma may have resulted from both the Deccan Trap eruptions and Chicxulub impact. Self et al. (2006, 2008) estimated that over ~13,000 Gt CO_2, was released from Deccan Traps emplacement during ~2 Ma, and the largest emission of CO_2 (~5000 Gt) also occurred over a short time-span (66.0–65.5 Ma) (Fig. 5). With respect to the current mass of atmospheric CO_2 (~3000 Gt), several single eruptive events spanning tens and hundreds of years, a mass of ~300 Gt degassing during each single eruptive event producing at least 40–80 ppmv in pCO_2 increase, is consistent with geochemical models of Caldeira and Rampino (1990) and the calculation from global volcanic emissions for thousands of years during the last deglaciation along with the current volcanic observations (Huybers and Langmuir, 2009). In contrast, Self et al. (2005) and Chenet et al. (2009) found much lower pCO_2 release from the Deccan Traps. Though the lavas contained little CO_2, vast amounts of CO_2 may

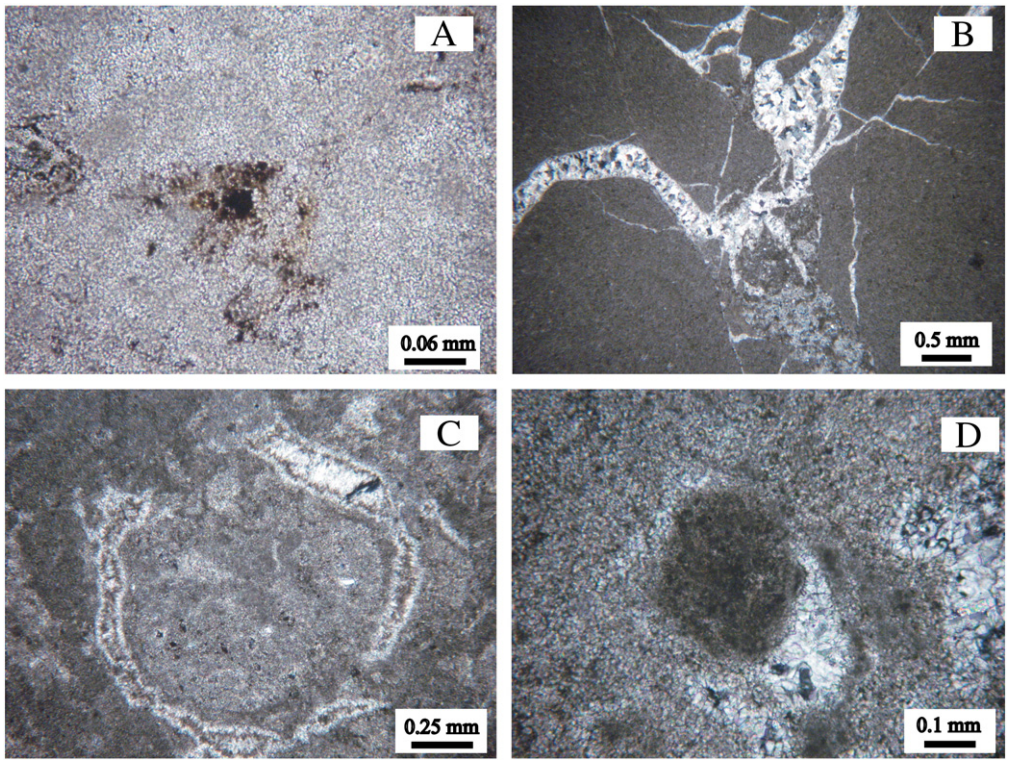

Fig. 4. Micrites in the carbonate nodules. A) Micritic fabrics (1320); B) micritic fabrics and sparry calcites in the cracks (298); C) micritic aggregates and circumgranular cracks cemented by microsparite (1350); and D) micrites and displacive fabrics (0971).

have been produced by contact metamorphism surrounding intrusions in carbonate rocks, coal or organic-rich shales (Ray et al., 2008; Ganino and Arndt, 2009; Hegde and Chavadi, 2009).

Presumably the Chicxulub impact at ~65.6 Ma contributed greatly to the input into the atmospheric CO_2. CO_2 produced from vaporized carbonates increased atmospheric CO_2 by a factor of 2 or more even for over 10^5 years because of the impact onto the carbonate-rich marine sedimentary terrace (O'Keefe and Ahrens, 1989; Beerling et al., 2002). The maximum amount of CO_2 was estimated at 100,000 Gt during the impact event (Takata and Ahrens, 1994). This is an unbelievably large amount, and is best regarded as a theoretical maximum, considering the complex kinetics and thermodynamics of the reactions during the impact events (Agrinier et al., 2001; Ivanov et al., 2002). Subsequent estimation from the numerical models and experiments, ranged from

Table 1
Data used to estimate paleoatmospheric CO_2 concentration across the K–T boundary from paleosols.

Age (Ma)	Sample no.	$\delta^{13}C_c$ (‰)	D_p (cm)	K (m)	D_c (cm)	P_r (ppmv)	$\delta^{13}C_r$ (‰)	$\delta^{13}O_c$ (‰)	T (°C)	$^{13}C_s$ (‰)	$\delta^{13}C_a$ (‰)	P_a (ppmv)	MP_a (ppmv)
63.1	0971	−9.02	60	0.269	62	4700	−25.2	−8.21	9.1	−19.70	−5.90	399±79	399±79
63.2	0980	−8.86	35	0.270	36	2987	−25.2	−7.36	10.8	−19.34	−5.90	341±103	341±103
64.1	1221	−9.11	30	0.297	31	2649	−25.3	−7.70	10.1	−19.67	−6.05	267±91	326±91
	1240	−8.93	50	0.299	52	4024	−25.3	−8.70	8.1	−19.73	−6.05	386±88	
64.2	1260	−8.35	10	0.300	10	1275	−25.3	−7.71	10.1	−18.92	−6.05	210±148	456±159
	1261	−8.05	40	0.301	41	3338	−25.3	−8.61	8.2	−18.83	−6.05	575±157	
	1262	−8.00	40	0.301	41	3338	−25.3	−8.72	8.0	−18.81	−6.05	582±159	
64.4	1320	−9.22	40	0.307	41	3339	−25.3	−8.03	9.4	−19.85	−6.05	286±78	286±78
64.5	1350	−8.27	40	0.311	41	3340	−25.3	−7.58	10.3	−18.81	−6.05	584±159	584±159
64.6	1370	−8.48	60	0.312	62	4717	−25.3	−8.56	8.3	−19.25	−6.05	640±126	451±126
	1381	−8.38	16	0.314	17	1689	−25.3	−8.02	9.4	−19.02	−6.050	263±140	
64.7	1391	−7.14	20	0.315	21	1965	−25.4	−7.3	10.9	−17.62	−6.10	592±271	569±271
	1400	−8.41	20	0.315	21	1965	−25.4	−7.41	10.7	−18.90	−6.10	336±154	
	1401	−8.06	20	0.315	21	1965	−25.4	−7.13	11.3	−18.49	−6.10	412±189	
	1410	−7.57	30	0.316	31	2653	−25.4	−8.59	8.3	−18.35	−6.10	593±202	
	1412	−8.12	60	0.316	62	4718	−25.4	−7.6	10.3	−18.66	−6.10	912±180	
64.9	1460	−7.56	30	0.321	31	2654	−24.9	−8.6	8.3	−18.35	−5.65	470±160	470±160
66.0	1890	−6.95	60	0.366	62	4738	−24.4	−9	7.4	−17.84	−5.18	837±164	837±164
67.8	2940	−7.51	30	0.477	31	2685	−24.0	−9.52	6.4	−18.52	−4.81	225±76	277±115
	2952	−7.07	20	0.478	21	1986	−24.0	−9.13	7.2	−17.99	−4.81	253±115	
	2953	−7.33	35	0.479	37	3034	−24.0	−9.31	6.8	−18.29	−4.81	310±93	
	2960	−7.38	40	0.479	42	3384	−24.0	−8.41	8.7	−18.12	−4.81	392±106	
	298	−7.17	26	0.480	27	2405	−24.0	−8.69	8.1	−17.98	−4.81	308±115	

Note: The standard errors of P_a are calculated using Gaussian error propagation; MP_a is the mean value of P_a at a certain age, and the standard errors of MP_a are assigned to the maximal P_a error at a certain age.

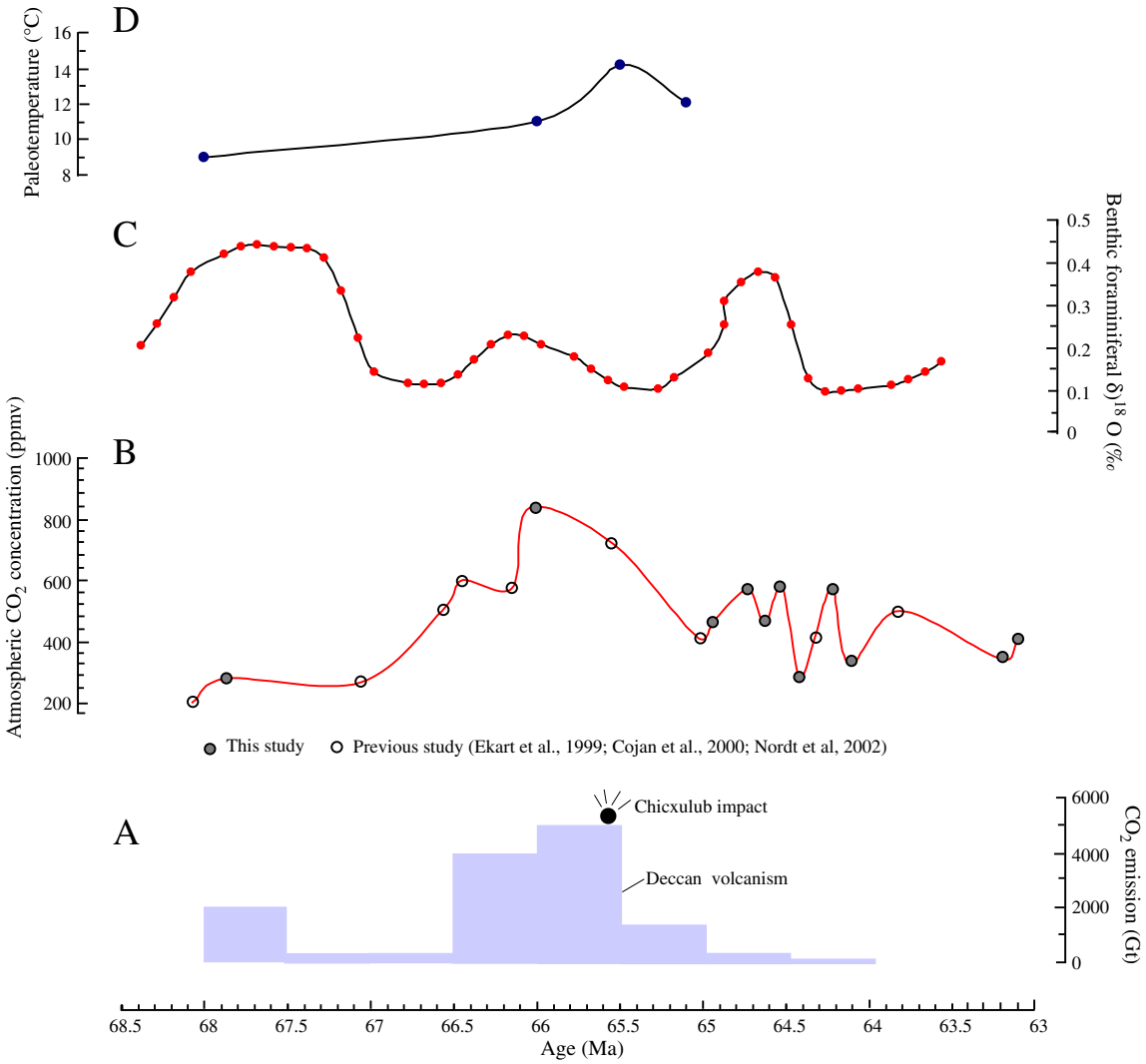

Fig. 5. A) Estimation on CO_2 mass erupted released from the Deccan traps, using a 0.5% mass fraction of CO_2 in flood basalt magmas (Self et al., 2006; Chenet et al., 2008, 2009) and the eruptive volumes and the age ranges of the main eruption phase after Self et al. (2006); B) an estimated atmospheric CO_2 across the K–T boundary from this study and previous paleosol barometer for pedogenic carbonates; C) benthic foraminiferal $\delta^{18}O$ trend for South Atlantic after Cramer et al. (2009); and D) paleotemperature calculated based on benthic foraminiferal $\delta^{18}O$ from Blake Nose Site 1050 after Huber et al. (2002).

~300 to $>10^4$ Gt for the mass of CO_2 emission into the atmosphere (Ivanov et al., 1996; Pope et al., 1997; Pierazzo et al., 1998; Kring and Durda, 2001; Beerling et al., 2002), is one to two orders of magnitude lower than that of Takata and Ahrens (1994). Despite disagreement concerning the mass of liberated CO_2, it is reasonable that the atmospheric pCO_2 level dramatically increased, due to vaporization of target rocks of the Chicxulub impact (Beerling et al., 2002; Premović, 2009).

Extensive wildfires ignited by the ejecta (Wolbach et al., 1990; Kring and Durda, 2002; Durda and Kring, 2004) or combustion of hydrocarbons during the impact event (Scott et al., 2000; Belcher et al., 2005; Harvey et al., 2008; Belcher et al., 2009) could introduce large amounts of CO_2 into the atmosphere (Kring, 2003, 2007). Nevertheless, the consequence of the impact-generated pulse of thermal radiation from these sources remains uncertain (Belcher et al., 2003; Belcher, 2009; Goldin and Melosh, 2009). Here we do not include the CO_2 emissions from above-mentioned processes, although ~10^4 Gt of CO_2-roughly equivalent to the mass of CO_2 liberated from vaporized target sediments, had been estimated (Kring and Durda, 2001; Kring, 2007).

In concert with the markedly elevated atmospheric CO_2 level, global warming, sea level rise and deglaciation should occur after a period of cooling resulting from the huge mass of dust and sulfate aerosols ejected from the impact (Kring, 2007; Huybers and Langmuir, 2009). Though the coupling of atmospheric CO_2 concentrations and climate change was suspected (Veizer et al., 2000; Kump, 2002; Shaviv and Veizer, 2003; Donnadieu et al., 2006), ocean temperature estimated from $\delta^{18}O$ of foraminifera disagreed with atmospheric pCO_2, perhaps due to seawater pH effects (Zeebe, 2001; Royer et al., 2004). However, other studies supported the hypothesis that global warming was driven by increased atmospheric pCO_2 level (Crowley and Berner, 2001; Pearson et al., 2001; Retallack, 2002; Royer et al., 2004; Came et al., 2007; Pucéat et al., 2007; Fletcher et al., 2008; Retallack, 2009a; Solomon et al., 2009, 2010). After a Late Cretaceous cooling (Pucéat et al., 2007), a global warming event occurred at the transition between late Maastrichtian and early Danian consistent with the elevated pCO_2, supported from the isotopes of numerous global drilling sites (Zachos et al., 1989; Li and Keller, 1998; Huber et al., 2002; Abramovich and Keller, 2003; Ravizza and Peucker-Ehrenbrink, 2003; MacLeod et al., 2005; Westerhold et al., 2011), simulation models (Pierazzo et al., 1998; Dessert et al., 2001; Hunter et al., 2008) and calcareous nannofossil assemblages (Thibault and Gardin, 2010). The seawater temperature estimates range from below 1 °C (Caldeira and Rampino, 1990), to ~2 °C (Pierazzo et al., 1998; Zachos et al., 2001; Huber et al., 2002),

4 °C or higher (Dessert et al., 2001; Beerling et al., 2002; Wilf et al., 2003).

A high-temporal-resolution curve of paleotemperature from the $\delta^{18}O$ of foraminifera in a duration corresponding to the K–T boundary is only known from the South Atlantic (Cramer et al., 2009). The $\delta^{18}O$ of foraminifera varied coincidently with the fluctuations of atmospheric CO_2 levels, even the smaller-scale CO_2 spike between 66 Ma and 67 Ma (Fig. 5). Recent progress in the high-resolution Maastrichtian and Paleocene stable isotope record from marine deposits reveals short-term global climate changes (Abramovich et al., 2010; Westerhold et al., 2011), for spikes of CO_2 input into the atmosphere less than occurred near the K–T boundary.

Sea level rise across the K–T boundary is known from sedimentary correlation of boreholes globally (Adatte et al., 2002; Miller et al., 2005a; Kominz, et al., 2008; Miller et al., 2011). Estimates of sea level fluctuation are less than 50 m (Haq et al., 1987; Miller et al., 2003; Van Sickel et al., 2004; Miller et al., 2005a,b; Kominz et al., 2008; Cramer et al., 2009; Miller et al., 2011). Furthermore, global seawater acidification and decreased $CaCO_3$ burial fluxes were observed at the K–T boundary due to the huge amount of CO_2-liberation induced by the Deccan volcanism and Chicxulub impact (Robinson et al., 2009; Premović, 2011) and impact generated nitric and sulfuric acid (Retallack, 1996).

7. Conclusions

Calcareous paleosols have been discovered in a scientific drill core from the Songliao Basin, northeast China. Well developed pedogenic carbonates were collected from the scientific drill core (SK-1 (N)). Here, we measured $\delta^{18}O$ and $\delta^{13}C$ values of these paleosol carbonates to estimate Cretaceous atmospheric pCO_2 levels using Cerling's (1991) model, as refined by Retallack (2009b).

Together with previous data on estimates of atmospheric pCO_2 from 67.8 Ma and 63.1 Ma, we found one large and several small pCO_2 spikes when CO_2 concentration rose from less than 300 ppmv between 68 Ma and 67 Ma to ~840 ppmv between 66.5 Ma and 65.5 Ma, then dropped and rose to ~550 ppmv between 64.7 Ma and 64.2 Ma.

Inconsistencies between various estimates of atmospheric CO_2 using the paleosol barometer can be largely ascribed to varied assumptions of different applications of the paleosol barometer and to differing temporal resolution of different paleosol sequences. Higher high-resolution records from pedogenic carbonates may provide insight into short-term spikes of paleo-atmospheric CO_2, as is demonstrated here to accompany mass extinction at the K–T boundary.

Rising pCO_2 after 66.5 Ma is consistent with the onset of main Deccan Trap eruptions, and atmospheric pCO_2 peaked within 66–65.5 Ma as a result of large eruption of the Deccan Traps in combination of masses of CO_2 released into the atmosphere produced from vaporized carbonates due to Chicxulub impact. The small CO_2 spikes between 64.7 Ma and 64.2 Ma derived from the CO_2-liberation from another phase of the Deccan Traps. Global warming and sea level rise was also associated with these CO_2 spikes.

Acknowledgments

C.M. Huang thanks Professor Pujun Wang of Jilin University for his assistance in sample collection from Drill SK-1 (N). This study was funded by the National Basic Research Program of China (973 Program) (grant no. 2012CB822003) and the Program for New Century Excellent Talents in University (grant no. NCET-08-0379).

References

Aberhan, M., Weidemeyer, S., Kiessling, W., Scasso, R.A., Medina, F.A., 2007. Faunal evidence for reduced productivity and uncoordinated recovery in Southern Hemisphere Cretaceous–Paleogene boundary sections. Geology 35, 227–230.

Abramovich, S., Keller, G., 2003. Planktonic foraminiferal response to the latest Maastrichtian abrupt warm event: a case study from South Atlantic DSDP Site 525A. Marine Micropaleontology 48, 225–249.

Abramovich, S., Yovel-Corem, S., Almogi-Labin, A., Benjamini, C., 2010. Global climate change and planktic foraminiferal response in the Maastrichtian. Paleoceanography 25, PA2201. http://dx.doi.org/10.1029/2009PA001843.

Adatte, T., Keller, G., Stinnesbeck, W., 2002. Late Cretaceous to early Paleocene climate and sea-level fluctuations: the Tunisian record. Palaeogeography, Palaeoclimatology, Palaeoecology 178, 178–196.

Agrinier, P., Deutsch, A., Schärer, U., Martinez, I., 2001. Fast back-reactions of shock-released CO_2 from carbonates: an experimental approach. Geochimica et Cosmochimica Acta 65, 2615–2632.

Alvarez, L.W., Alvarez, W., Asaro, F., Michel, H.V., 1980. Extraterrestrial cause for the Cretaceous–Tertiary extinction. Science 208, 1095–1108.

Archibald, J.D., Clemens, W.A., Padian, K., Rowe, T., Macleod, N., Barrett, P.M., Gale, A., Holroyd, P., Sues, H.D., Arens, N.C., Horner, J.R., Wilson, G.P., Goodwin, M.B., Brochu, C.A., Lofgren, D.L., Hurlbert, S.H., Hartman, J.H., Eberth, D.A., Wignall, P.B., Currie, P.J., Weil, A., Prasad, G.V., Dingus, L., Courtillot, V., Milner, A., Milner, A., Bajpai, S., Ward, D.J., Sahni, A., 2010. Cretaceous extinctions: multiple causes. Science 328, 973.

Arens, N.C., Jahren, A.H., 2002. Chemostratigraphic correlation of four fossil-bearing sections in southwestern North Dakota. In: Hartman, J.H., Johnson, K.R., Nichols, D.J. (Eds.), The Hell Creek Formation and the Cretaceous–Tertiary Boundary in the Northern Great Plains: An Integrated Continental Record of the End of the Cretaceous: Geological Society of America Special Paper, 361, pp. 75–93.

Arens, N.C., Jahren, A.H., Amundson, R., 2000. Can C3 plants faithfully record the carbon isotopic composition of atmospheric carbon dioxide? Paleobiology 26, 137–164.

Beerling, D.J., Lomax, B.H., Royer, D.L., Upchurch, G.R., Kump, L.R., 2002. An atmospheric pCO_2 reconstruction across the Cretaceous–Tertiary boundary from leaf megafossils. Proceedings of the National Academy of Sciences of the United States of America 99, 7836–7840.

Belcher, C.M., 2009. Reigniting the Cretaceous–Palaeogene firestorm debate. Geology 37, 1147–1148.

Belcher, C.M., Collinson, M.E., Sweet, A.R., Hildebrand, A.R., Scott, A.C., 2003. Fireball passes and nothing burns—the role of thermal radiation in the Cretaceous–Tertiary event: evidence from the charcoal record of North America. Geology 31, 1061–1064.

Belcher, C.M., Collinson, M.E., Scott, A.C., 2005. Constraints on the thermal energy released from the Chicxulub impactor: new evidence from multimethod charcoal analysis. Journal of the Geological Society of London 162, 591–602.

Belcher, C.M., Finch, P., Collinson, M.E., Scott, A.C., Grassineau, N.V., 2009. Geochemical evidence for combustion of hydrocarbons during the K–T impact event. Proceedings of the National Academy of Sciences of the United States of America 106, 4112–4117.

Berner, R.A., 2006. GEOCARBSULF: a combined model for Phanerozoic atmospheric O_2 and CO_2. Geochimica et Cosmochimica Acta 70, 5653–5664.

Berner, R.A., Kothavala, Z., 2001. GEOCARB III: a revised model of atmospheric CO_2 over Phanerozoic time. American Journal of Science 301, 182–204.

Braman, D.R., Sweet, A.R., 1999. Terrestrial palynomorph biostratigraphy of the Cypress Hills, Wood Mountain, and Turtle Mountain areas (Upper Cretaceous–Paleocene) of western Canada. Canadian Journal of Earth Sciences 36, 725–741.

Breecker, D.O., Sharp, Z.D., McFadden, L.D., 2010. Atmospheric CO_2 concentrations during ancient greenhouse climates were similar to those predicted for A.D. 2100. Proceedings of the National Academy of Sciences of the United States of America 107, 576–580.

Bryan, S.E., Peate, I.U., Peate, D.W., Self, S., Jerram, D.A., Mawby, M.R., Marsh, J.S., Miller, J.A., 2010. The largest volcanic eruptions on Earth. Earth-Science Reviews 102, 207–229.

Budd, D.A., Pack, S.M., Fogel, M.L., 2002. The destruction of paleoclimatic isotropic signals in Pleistocene carbonate soil nodules of Western Australia. Palaeogeography, Palaeoclimatology, Palaeoecology 188, 249–273.

Caldeira, K., Rampino, M.R., 1990. Carbon dioxide emissions from Deccan volcanism and a K/T boundary greenhouse effect. Geophysical Research Letters 17, 1299–1302.

Came, R.E., Eiler, J.M., Veizer, J., Azmy, K., Brand, U., Weidman, C.R., 2007. Coupling of surface temperatures and atmospheric CO_2 concentrations during the Palaeozoic era. Nature 449, 198–201.

Cande, S., Kent, D.V., 1995. Revised calibration of the geomagnetic polarity timescale for the Late Cretaceous and Cenozoic. Journal of Geophysical Research 100, 6093–6095.

Cerling, T.E., 1984. The stable isotopic composition of modern soil carbonate and its relationship to climate. Earth and Planetary Science Letters 71, 229–240.

Cerling, T.E., 1991. Carbon dioxide in the atmosphere: evidence from Cenozoic and Mesozoic paleosols. American Journal of Science 291, 377–400.

Cerling, T.E., 1999. Stable carbon isotopes in paleosol carbonates. In: Thirty, M., Coincon, R. (Eds.), Palaeoweathering, Palaeosurfaces, and Related Continental Deposits: International Association of Sedimentologist Special Publication, 27, pp. 43–60.

Cerling, T.E., Quade, J., 1993. Stable carbon and oxygen isotopes in soil carbonates. In: Swart, P.K., Lohmann, K.C., McKenzie, J.A., Savin, S.M. (Eds.), Climate Change in Continental Isotopic Records: American Geophysical Union Geophysical Monograph, 78, pp. 217–231.

Chen, P.J., Wan, X.Q., Jiang, J.H., Li, X.H., Cao, L., Li, G., Liu, J.C., Yin, D.S., Yan, W., Li, W.X., 2004. Searching for the strato-type of the Furaoan Stage in Heilongjiang Province, northeast China. Journal of Stratigraphy 28 (2), 97–103 (in Chinese, English abstract).

Chenet, A.L., Quidelleur, X., Fluteau, F., Courtillot, V., 2007. ^{40}K–^{40}Ar dating of the main Deccan large igneous province: further evidence of KTB age and short duration. Earth and Planetary Science Letters 263, 1–15.

Chenet, A.L., Fluteau, F., Courtillot, V., Gérard, M., Subbarao, K.V., 2008. Determination of rapid Deccan eruptions across the Cretaceous–Tertiary boundary using paleomagnetic secular variation: results from a 1200-m-thick section in the Mahabaleshwar escarpment. Journal of Geophysical Research 113, B04101. http://dx.doi.org/10.1029/2006JB004635.

Chenet, A.L., Courtillot, V., Fluteau, F., Gérard, M., Quidelleur, X., Khadri, S.F.R., Subbarao, K.V., Thordarson, T., 2009. Determination of rapid Deccan eruptions across the Cretaceous–Tertiary boundary using paleomagnetic secular variation: 2. Constraints from analysis of eight new sections and synthesis for a 3500-m-thick composite section. Journal of Geophysical Research 114, B06103. http://dx.doi.org/10.1029/2008JB005644.

Claeys, P., Kiessling, W., Alvarez, W., 2002. Distribution of Chicxulub ejecta at the Cretaceous–Tertiary boundary. In: Koeberl, C., MacLeod, K.G. (Eds.), Catastrophic Events and Mass Extinctions: Impacts and Beyond: Geological Society of America Special Paper, 356, pp. 55–68.

Cleveland, D.M., Nordt, L.C., Dworkin, S.I., Atchley, S.C., 2008a. Pedogenic carbonate isotopes as evidence for extreme climatic events preceding the Triassic–Jurassic boundary: implications for the biotic crisis? Geological Society of America Bulletin 120, 1408–1415.

Cleveland, D.M., Nordt, L.C., Atchley, S.C., 2008b. Paleosols, trace fossils, and precipitation estimates of the uppermost Triassic strata in northern New Mexico. Palaeogeography, Palaeoclimatology, Palaeoecology 257, 421–444.

Cojan, L., Moreau, M.G., Stott, L., 2000. Stable isotope stratigraphy of the Paleogene pedogenic series of southern France as a basis for continental–marine correlation. Geology 28, 259–262.

Cotton, J.M., Sheldon, N.D., 2012. New constraints on using paleosols to reconstruct atmospheric pCO_2. Geological Society of America Bulletin 124, 1411–1423.

Courtillot, V., Fluteau, F., 2010. Cretaceous extinctions: the volcanic hypothesis. Science 328, 973–974.

Courtillot, V., Besse, J., Vandamme, D., Montigny, R., Jaeger, J.J., Capetta, H., 1986. Deccan flood basalts at the Cretaceous/Tertiary boundary. Earth and Planetary Science Letters 80, 361–374.

Cramer, B.S., Toggweiler, J.R., Wright, J.D., Katz, M.E., Miller, K.G., 2009. Ocean overturning since the Late Cretaceous: inferences from a new benthic foraminiferal isotope compilation. Paleoceanography 24, PA4216. http://dx.doi.org/10.1029/2008PA001683.

Crowley, T.J., Berner, R.A., 2001. CO_2 and climate change. Science 292, 870–872.

D'Hondt, S., Donaghay, P., Zachos, J.C., Luttenberg, D., Lindinger, M., 1998. Organic carbon fluxes and ecological recovery from Cretaceous–Tertiary mass extinction. Science 282, 276–279.

Deng, C.L., He, H.Y., Pan, Y.X., Zhu, R.X., 2013. Chronology of the terrestrial Upper Cretaceous in the Songliao Basin, northeast Asia. Palaeogeography Palaeoclimatology Palaeoecology 385, 44–54.

Dessert, C., Dupré, B., François, L.M., Schott, J., Gaillardet, J., Chakrapani, G.J., Bajpai, S., 2001. Erosion of Deccan Traps determined by river geochemistry: impact on the global climate and the $^{87}Sr/^{86}Sr$ ratio of seawater. Earth and Planetary Science Letters 188, 459–474.

Deutz, P., Montañez, I.P., Monger, H.C., 2002. Morphology and stable and radiogenic isotope composition of pedogenic carbonates in Late Quaternary relict soils, New Mexico, U.S.A.: an integrated record of pedogenic overprinting. Journal of Sedimentary Research 72, 809–822.

Donnadieu, Y., Pierrehumbert, R., Jacob, R., Fluteau, F., 2006. Modelling the primary control of paleogeography on Cretaceous climate. Earth and Planetary Science Letters 248, 426–437.

Duncan, R.A., Pyle, D.G., 1988. Rapid eruption of the Deccan flood basalts at the Cretaceous/Tertiary boundary. Nature 333, 841–843.

Durda, D.D., Kring, D.A., 2004. Ignition threshold for impact generated fires. Journal of Geophysical Research 109, E08004. http://dx.doi.org/10.1029/2004JE002279.

Dworkin, S.I., Nordt, L., Atchley, S., 2005. Determining terrestrial paleotemperatures using the oxygen isotopic composition of pedogenic carbonate. Earth and Planetary Science Letters 237, 56–68.

Ekart, D.D., Cerling, T.E., Montañez, I.P., Tabor, N.J., 1999. 400 million year carbon isotope record of pedogenic carbonate: implications for paleoatmospheric carbon dioxide. American Journal of Science 299, 805–827.

Fischer, H., Wahlen, M., Smith, J., Mastroianni, D., Deck, B., 1999. Ice core records of atmospheric CO_2 around the last three glacial terminations. Science 283, 1712–1714.

Fletcher, B.J., Brentnall, S.J., Anderson, C.W., Berner, R.A., Beerling, D.J., 2008. Atmospheric carbon dioxide linked with Mesozoic and early Cenozoic climate change. Nature Geoscience 1, 43–48.

Ganino, C., Arndt, N.T., 2009. Climate changes caused by degassing of sediments during the emplacement of large igneous provinces. Geology 37, 323–326.

Gao, R.Q., Zhang, Y., Cui, T.C., 1994. Cretaceous Petroleum Bearing Strata in the Songliao Basin. Petroleum Industry Press, Beijing (333 pp., in Chinese).

Goldin, T.J., Melosh, H.J., 2009. Self-shielding of thermal radiation by Chicxulub impact ejecta: firestorm or fizzle? Geology 37, 1135–1138.

Goudie, A.S., 1983. Calcretes. In: Goudie, A.S., Pye, K. (Eds.), Chemical Sediments and Geomorphology: Precipitates and Residua in the Near-surface Environment. Academic Press, London, pp. 93–132.

Haq, B.U., Hardenbol, J., Vail, P.R., 1987. Chronology of fluctuating sea levels since the Triassic. Science 235, 1156–1167.

Harvey, M.C., Brassell, S.C., Belcher, C.M., Montanari, A., 2008. Combustion of fossil organic matter at the Cretaceous–Paleogene (K–P) boundary. Geology 36, 355–358.

Hasegawa, T., Pratt, L.M., Maeda, H., Shigeta, Y., Okamoto, T., Kase, T., Uemura, K., 2003. Upper Cretaceous stable carbon isotope stratigraphy of terrestrial organic matter from Sakhalin, Russian Far East: a proxy for the isotopic composition of paleoatmospheric CO_2. Palaeogeography, Palaeoclimatology, Palaeoecology 189, 97–115.

Hegde, V.S., Chavadi, V.C., 2009. Geochemistry of late Archaean metagreywackes from the Western Dharwar Craton, South India: implications for provenance and nature of the Late Archaean crust. Gondwana Research 15, 178–187.

Hildebrand, A.R., Penfield, G.T., Kring, D.A., Pilkington, M., Zanoguera, A.C., Jacobsen, S.B., Boynton, W.V., 1991. Chicxulub Crater: a possible Cretaceous/Tertiary boundary impact crater on the Yucatán Peninsula, Mexico. Geology 19, 867–871.

Hooper, P., Widdowson, M., Kelley, S., 2010. Tectonic setting and timing of the final Deccan flood basalt eruptions. Geology 38, 839–842.

Huang, C.M., Retallack, G.J., Wang, C.S., 2010. Cretaceous calcareous paleosols: pedogenetic characteristics and paleoenvironmental implications. Acta Pedologica Sinica 47, 1029–1038 (in Chinese, English abstract).

Huber, B.T., Norris, R.D., MacLeod, K.G., 2002. Deep-sea paleotemperature record of extreme warmth during the Cretaceous. Geology 30, 123–126.

Hunter, S.J., Valdes, P.J., Haywood, A.M., Markwick, P.J., 2008. Modelling Maastrichtian climate: investigating the role of geography, atmospheric CO_2 and vegetation. Climate of the Past Discussions 4, 981–1019.

Huybers, P., Langmuir, C., 2009. Feedback between deglaciation, volcanism, and atmospheric CO_2. Earth and Planetary Science Letters 286, 479–491.

Ivanov, B.A., Badjukov, O.I., Yakovlev, M.I., Gerasimov, M.V., Dikov, Y.P., Pope, K.O., Ocampo, A.C., 1996. Degassing of sedimentary rocks due to Chicxulub impact: hydrocode and physical simulations. In: Ryder, G., Fastovsky, D., Gartner, S. (Eds.), The Cretaceous–Tertiary Event and Other Catastrophes in Earth History: Geological Society of America Special Paper, 307, pp. 125–139.

Ivanov, B.A., Langenhorst, F., Deutsch, A., Hornemann, U., 2002. How strong was impact-induced CO_2 degassing in the Cretaceous–Tertiary event? Numerical modeling of shock recovery experiments. Geological Society of America Special Paper 356, 587–594.

Ivany, L.C., Salawitch, R.J., 1993. Carbon isotopic evidence for biomass burning at the K/T boundary. Geology 21, 487–490.

Jay, A.E., Niocaill, C.M., Widdowson, M., Self, S., Turner, W., 2009. New palaeomagnetic data from the Mahabaleshwar Plateau, Deccan Flood Basalt Province, India: implications for the volcanostratigraphic architecture of continental flood basalt provinces. Journal of the Geological Society of London 166, 13–24.

Jones, T.P., Lim, B., 2000. Extraterrestrial impacts and wildfires. Palaeogeography, Palaeoclimatology, Palaeoecology 164, 57–66.

Keller, G., 2001. The end-Cretaceous mass extinction: year 2000 assessment. Planetary and Space Science 49, 817–830.

Keller, G., Stinnesbeck, W., Adatte, T., Stüben, D., 2003. Multiple impacts across the Cretaceous–Tertiary boundary. Earth-Science Reviews 62, 327–363.

Keller, G., Adatte, T., Gardin, S., Bartolini, A., Bajpai, S., 2008. Main Deccan volcanism phase ends near the K–T boundary: evidence from the Krishna-Godavari Basin, SE India. Earth and Planetary Science Letters 268, 293–311.

Keller, G., Sahni, A., Bajpai, S., 2009. Deccan volcanism, the KT mass extinction and dinosaurs. Journal of Biosciences 34, 709–728.

Keller, G., Adatte, T., Pardo, A., Bajpai, S., Khosla, A., Samant, B., 2010. Cretaceous extinctions: evidence overlooked. Science 328, 974–975.

Kominz, M.A., Browning, J.V., Miller, K.G., Sugarman, P.J., Misintseva, S., Scotese, C.R., 2008. Late Cretaceous to Miocene sea-level estimates from the New Jersey and Delaware coastal plain coreholes: an error analysis. Basin Research 20, 211–226.

Kovda, I.V., Wilding, L.P., Drees, L.R., 2003. Micromorphology, submicroscopy and microprobe study of carbonate pedofeatures in a Vertisol gilgai soil complex, South Russia. Catena 54, 457–476.

Kring, D.A., 2003. Environmental consequences of impact cratering events as a function of ambient conditions on Earth. Astrobiology 3, 133–152.

Kring, D.A., 2007. The Chicxulub impact event and its environmental consequences at the Cretaceous–Tertiary boundary. Palaeogeography, Palaeoclimatology, Palaeoecology 255, 4–21.

Kring, D.A., Durda, D.D., 2001. The distribution of wildfires ignited by high-energy ejecta from the Chicxulub impact event. Lunar Planetary Science XXXII.Lunar and Planetary Institute, Houston, TX (Abstract #1447, CD-ROM).

Kring, D.A., Durda, D.D., 2002. Trajectories and distribution of material ejected from the Chicxulub impact crater: implications for postimpact wildfires. Journal of Geophysical Research 107 (E8), 5062. http://dx.doi.org/10.1029/2001JE001532.

Kump, L.R., 2002. Reducing uncertainty about carbon dioxide as a climate driver. Nature 419, 188–190.

Li, L., Keller, G., 1998. Maastrichtian climate, productivity and faunal turnovers in planktic foraminifera in South Atlantic DSDP sites 525A and 21. Marine Micropaleontology 33, 55–86.

Li, X.H., Li, W.X., Chen, P.J., Wan, X.Q., Li, G., Song, B., Jiang, J.H., Liu, J.C., Yin, D.S., Yan, W., 2004. SHRIMP U–Pb zircon dating of the uppermost Cretaceous Furao Formation near the Heilong River: an age closest to the K/T boundary. Chinese Science Bulletin 49, 860–862.

Li, J.G., Batten, D.J., Zhang, Y.Y., 2011. Palynological record from a composite core through Late Cretaceous–early Paleocene deposits in the Songliao Basin, Northeast China and its biostratigraphic implications. Cretaceous Research 32, 1–12.

Liu, G.W., Braman, D.R., Li, W.T., Brinkman, D., 2009. Palynostratigraphic characteristics of Cretaceous–Paleogene boundary of western-north America and review on searching for Cretaceous–Paleogene boundary in eastern China. Journal of Stratigraphy 33, 17–34 (in Chinese, English abstract).

Lourantou, A., Chappellaz, J., Barnola, J.M., Masson-Delmotte, V., Raynaud, D., 2010. Changes in atmospheric CO_2 and its carbon isotopic ratio during the penultimate deglaciation. Quaternary Science Reviews 29, 1983–1992.

Lüthi, D., Floch, M.L., Bereiter, B., Blunier, T., Barnola, J.M., Siegenthaler, U., Raynaud, D., Jouzel, J., Fischer, H., Kawamura, K., Stocker, T.F., 2008. High-resolution carbon dioxide concentration record 650,000–800,000 years before present. Nature 453, 379–382.

Mack, G.H., Cole, D.R., 2005. Geochemical model of $\delta^{18}O$ of pedogenic calcite versus latitude and its application to Cretaceous palaeoclimate. Sedimentary Geology 174, 115–122.

MacLeod, N., 2003. The causes of Phanerozoic extinctions. In: Rothschild, L., Lister, A. (Eds.), Evolution on Planet Earth. Academic Press, London, pp. 253–277.

MacLeod, K.G., Huber, B.T., Isaza, C., 2005. North Atlantic warming during "global" cooling at the end of the Cretaceous. Geology 33, 437–440.

MacLeod, K.G., Whitney, D.L., Huber, B.T., Koeberl, C., 2007. Impact and extinction in remarkably complete Cretaceous–Tertiary boundary sections from Demerara Rise, tropical western North Atlantic. Geological Society of America Bulletin 119, 101–115.

Maruoka, T., Koeberl, C., Bohor, B.F., 2007. Carbon isotopic compositions of organic matter across continental Cretaceous–Tertiary (K–T) boundary sections: implications for paleoenvironment after the K–T impact event. Earth and Planetary Science Letters 253, 226–238.

Melosh, H.J., Schneider, N.M., Zahnle, K.J., Latham, D., 1990. Ignition of global wildfires at the Cretaceous/Tertiary boundary. Nature 343, 251–254.

Miller, K.G., Sugarman, P.J., Browning, J.V., Kominz, M.A., Hernández, J.C., Olsson, R.K., Wright, J.D., Feigenson, M.D., Van Sickel, W., 2003. Late Cretaceous chronology of large, rapid sea level changes: glacioeustasy during the greenhouse world. Geology 31, 585–588.

Miller, K.G., Kominz, M.A., Browning, J.V., Wright, J.D., Mountain, G.S., Katz, M.E., Sugarman, P.J., Cramer, B.S., Christie-Blick, N., Pekar, S.F., 2005a. The Phanerozoic record of global sea-level change. Science 310, 1293–1298.

Miller, K.G., Wright, J.D., Browning, J.V., 2005b. Visions of ice sheets in a greenhouse world. Marine Geology 217, 215–231.

Miller, K.G., Sherrell, R.M., Browning, J.V., Field, M.P., Gallagher, W., Olsson, R.K., Sugarman, P.J., Tuorto, S., Wahyudi, H., 2010. Relationship between mass extinction and iridium across the Cretaceous–Paleogene boundary in New Jersey. Geology 38, 867–870.

Miller, K.G., Mountain, G.S., Wright, J.D., Browning, J.V., 2011. A 180-million-year record of sea level and ice volume variations from continental margin and deep-sea isotopic records. Oceanography 24 (2), 40–53.

Nichols, D.J., 1990. Geologic and biostratigraphic framework of the non-marine Cretaceous–Tertiary boundary interval in western North America. Review of Palaeobotany and Palynology 65, 75–84.

Nordt, L., Atchley, S., Dworkin, S.I., 2002. Paleosol barometer indicates extreme fluctuations in atmospheric CO_2 across the Cretaceous–Tertiary boundary. Geology 2002 (30), 703–706.

Nordt, L., Atchley, S., Dworkin, S.I., 2003. Terrestrial evidence for two greenhouse events in the latest Cretaceous. GSA Today 13 (12), 4–9.

O'Keefe, J.D., Ahrens, T.J., 1989. Impact production of CO_2 by the Cretaceous–Tertiary extinction bolide and the resultant heating of the Earth. Nature 338, 247–249.

Officer, C.B., Hallam, A., Drake, C.L., Devine, J.D., 1987. Late Cretaceous and paroxysmal Cretaceous/Tertiary extinctions. Nature 326, 143–149.

Pan, Y.Y., Huang, C.M., 2012. Quantitative reconstruction of the Early Cretaceous paleoclimate using paleosol carbonates in China.

Passey, B.H., Cerling, T.E., Perkins, M.E., Voorhies, M.R., Harris, J.M., Tucker, S.T., 2002. Environmental change in the Great Plains: an isotopic record from fossil horses. Journal of Geology 110, 123–140.

Pearson, P.N., Ditchfield, P.W., Singano, J., Harcourt-Brown, K.G., Nicholas, C.J., Olsson, R.K., Shackleton, N.J., Hall, M.A., 2001. Warm tropical sea surface temperatures in the Late Cretaceous and Eocene epochs. Nature 413, 481–488.

Peters, S.E., 2008. Environmental determinants of extinction selectivity in the fossil record. Nature 454, 626–629.

Petit, J.R., Jouzel, J., Raynaud, D., Barkov, N.I., Barnola, J.M., Basile, I., Bender, M., Chappellaz, J., Davis, M., Delaygue, G., Delmotte, M., Kotlyakov, V.M., Legrand, M., Lipenkov, V.Y., Lorius, C., Pepin, L., Ritz, C., Saltzman, E., Stievenard, M., 1999. Climate and atmospheric history of the past 420,000 years from the Vostok ice core, Antarctica. Nature 399, 429–436.

Pierazzo, E., Kring, D.A., Melosh, H.J., 1998. Hydrocode simulation of the Chicxulub impact event and the production of climatically active gases. Journal of Geophysical Research 103, 28607–28625.

Pope, K., Baines, K., Ocampo, A., Ivanov, B., 1997. Energy, volatile production, and climatic effects of the Chicxulub Cretaceous/Tertiary impact. Journal of Geophysical Research 102 (E9), 21645–21664.

Premović, P.I., 2009. Experimental evidence for the global acidification of surface ocean at the Cretaceous–Palaeogene boundary: the biogenic calcite-poor spherule layers. International Journal of Astrobiology 8, 193–206.

Premović, P.I., 2011. Distal "impact" layers and global acidification of ocean water at the Cretaceous–Paleogene boundary (KPB). Geochemistry International 49, 55–65.

Prochnow, S.J., Nordt, L.C., Atchley, S.C., Hudec, M.R., 2006. Multi-proxy paleosol evidence for middle and late Triassic climate trends in eastern Utah. Palaeogeography, Palaeoclimatology, Palaeoecology 232, 53–72.

Pucéat, E., Lécuyer, C., Donnadieu, Y., Naveau, P., Cappetta, H., Ramstein, G., Huber, B.T., Kriwet, J., 2007. Fish tooth $\delta^{18}O$ revising Late Cretaceous meridional upper ocean water temperature gradients. Geology 35, 107–110.

Quade, J., Cerling, T.E., Bowman, J.R., 1989. Development of Asian monsoon revealed by marked ecological shift during the latest Miocene in northern Pakistan. Nature 342, 162–166.

Quan, C., Sun, G., Zhou, Z.Y., 2010. A new Tertiary *Ginkgo* (Ginkgoaceae) from the Wuyun Formation of Jiayin, Heilongjiang, northeastern China and its paleoenvironmental implications. American Journal of Botany 97, 446–457.

Quast, A., Hoefs, J., Paul, J., 2006. Pedogenic carbonates as a proxy for palaeo-CO_2 in the Palaeozoic atmosphere. Palaeogeography, Palaeoclimatology, Palaeoecology 242, 110–125.

Ravizza, G., Peucker-Ehrenbrink, B., 2003. Chemostratigraphic evidence of Deccan volcanism from the marine osmium isotope record. Science 302, 1392–1395.

Ray, R., Shukla, A.D., Sheth, H.C., Ray, J.S., Duraiswami, R.A., Vanderkluysen, L., Rautela, C.S., Mallik, J., 2008. Highly heterogeneous Precambrian basement under the central Deccan Traps, India: direct evidence from xenoliths in dykes. Gondwana Research 13, 375–385.

Retallack, G.J., 1996. Acid trauma at the Cretaceous–Tertiary boundary in eastern Montana. GSA Today 6 (5), 1–7.

Retallack, G.J., 1997. A Colour Guide to Paleosols. John Wiley, New York, pp. 29–112.

Retallack, G.J., 2001. Soils of the Past—An Introduction to Paleopedology. Blackwell Science Ltd., Oxford (333 pp.).

Retallack, G.J., 2002. Carbon dioxide and climate over the past 300 Myr. Philosophical Transactions of the Royal Society of London. Series A 360, 659–673.

Retallack, G.J., 2004. End-Cretaceous acid rain as a selective extinction mechanism between birds and dinosaurs. In: Currie, P.J., Koppelhus, E.B., Shugar, M.A., Wright, J.L. (Eds.), Feathered Dragons: Studies on the Transition from Dinosaurs to Birds. Indiana University Press, Bloomington and Indianapolis, pp. 35–64.

Retallack, G.J., 2009a. Greenhouse crises of the past 300 million years. Geological Society of America Bulletin 121, 1441–1455.

Retallack, G.J., 2009b. Refining a pedogenic–carbonate CO_2 paleobarometer to quantify a middle Miocene greenhouse spike. Palaeogeography, Palaeoclimatology, Palaeoecology 281, 57–65.

Robinson, S.A., Andrews, J.E., Hesselbo, S.P., Radley, J.D., Dennis, P.F., Harding, I.C., Allen, P., 2002. Atmospheric pCO_2 and depositional environment from stable-isotope geochemistry of calcrete nodules (Barremian, Lower Cretaceous, Wealden Beds, England). Journal of the Geological Society of London 159, 215–224.

Robinson, N., Ravizza, G., Coccioni, R., Peucker-Ehrenbrink, B., Norris, R., 2009. A high-resolution marine $^{187}Os/^{188}Os$ record for the late Maastrichtian: distinguishing the chemical fingerprints of Deccan volcanism and the KP impact event. Earth and Planetary Science Letters 281, 159–168.

Romanek, C., Grossman, E., Morse, J., 1992. Carbon isotopic fractionation in synthetic aragonite and calcite: effects of temperature and precipitation rate. Geochimica et Cosmochimica Acta 56, 419–430.

Royer, D.L., 2010. Fossil soils constrain ancient climate sensitivity. Proceedings of the National Academy of Sciences of the United States of America 107, 517–518.

Royer, D.L., Berner, R.A., Beerling, D.J., 2001. Phanerozoic atmospheric CO_2 change: evaluating geochemical and paleobiological approaches. Earth-Science Reviews 54, 349–392.

Royer, D.L., Berner, R.A., Montañez, I.P., Tabor, N.J., Beerling, D.J., 2004. CO_2 as a primary driver of Phanerozoic climate. GSA Today 14 (3), 4–10.

Schulte, P., Alegret, L., Arenillas, I., et al., 2010. The Chicxulub asteroid impact and mass extinction at the Cretaceous–Paleogene boundary. Science 327, 1214–1218.

Scotese, C.R., Gahagan, L., Larson, R.L., 1988. Plate tectonic reconstruction of the Cretaceous and Cenozoic ocean basins. Tectonophysics 155, 27–48.

Scott, A.C., Lomax, B.H., Collinson, M.E., Upchurch, G.R., Beerling, D.J., 2000. Fire across the K–T boundary: initial results from the Sugarite Coal, New Mexico, USA. Palaeogeography, Palaeoclimatology, Palaeoecology 164, 381–395.

Self, S., Thordarson, T., Widdowson, M., 2005. Gas fluxes from flood basalt eruptions. Elements 1, 283–287.

Self, S., Thordarson, T., Widdowson, M., Jay, A.E., 2006. Volatile fluxes during flood basalt eruptions and potential effects on the global environment: a Deccan perspective. Earth and Planetary Science Letters 248, 518–532.

Self, S., Jay, A.E., Widdowson, M., Keszthelyi, L.P., 2008. Correlation of the Deccan and Rajahmundry Trap lavas: are these the longest and largest lava flows on Earth? Journal of Volcanology and Geothermal Research 172, 3–19.

Shackleton, N., Bleil, U., 1985. Carbon-isotope stratigraphy, Site 577. In: Turner, K. (Ed.), Initial report of the Deep Sea Drilling Project. U.S. Government Printing Office, Washington, D.C., vol. 86. pp. 503–511.

Shaviv, N.J., Veizer, J., 2003. Celestial driver of Phanerozoic climate? GSA Today 13 (7), 4–10.

Sheldon, N.D., Retallack, G.J., 2001. Equation for compaction of paleosols due to burial. Geology 29, 247–250.

Sheldon, N.D., Retallack, G.J., Tanaka, S., 2002. Geochemical climofunctions from North America soils and application to paleosols across the Eocene–Oligocene boundary in Oregon. Journal of Geology 110, 687–696.

Siegenthaler, U., Stocker, T.F., Monnin, E., Lüthi, D., Schwander, J., Stauffer, B., Raynaud, D., Barnola, J.M., Fischer, H., Masson-Delmotte, V., Jouzel, J., 2005. Stable carbon cycle–climate relationship during the Late Pleistocene. Science 310, 1313–1317.

Solomon, S., Plattner, G.K., Knutti, R., Friedlingstein, P., 2009. Irreversible climate change due to carbon dioxide emissions. Proceedings of the National Academy of Sciences of the United States of America 106, 1704–1709.

Solomon, S., Daniel, J.S., Sanford, T.J., Murphy, D.M., Plattner, G.-K., Knutti, R., Friedlingstein, P., 2010. Persistence of climate changes due to a range of greenhouse gases. Proceedings of the National Academy of Sciences of the United States of America 107, 18354–18359.

Sweet, A.R., Braman, D.R., 2001. Cretaceous–Tertiary palynofloral perturbations and extinctions within the *Aquilapollenites* Phytogeographic Province. Canadian Journal of Earth Sciences 38, 249–269.

Tabor, N.J., Montañez, I.P., 2005. Oxygen and hydrogen isotope compositions of Permian pedogenic phyllosilicates: development of modern surface domain arrays and implications for paleotemperature reconstructions. Palaeogeography, Palaeoclimatology, Palaeoecology 223, 127–146.

Tajika, E., 1999. Carbon cycle and climate change during the Cretaceous inferred from a biogeochemical carbon cycle model. The Island Arc 8, 293–303.

Takata, T., Ahrens, T.J., 1994. Numerical simulation of impact cratering at Chicxulub and the possible causes of KT catastrophe (abstract). New Developments Regarding the KT Event and Other Catastrophes in Earth History. LPI Contribution, 825. Lunar and Planetary Institute, Houston, pp. 125–126.

Therrien, F., Eberth, D.A., Braman, D.R., Zelenitsky, D.K., 2007. High-resolution organic carbon isotope record across the Cretaceous–Tertiary boundary in south-central Alberta: implications for the post-impact recovery rate of terrestrial ecosystems and use of $\delta^{13}C$ as a boundary tracer. Canadian Journal of Earth Sciences 44, 529–542.

Thibault, N., Gardin, S., 2010. The calcareous nannofossil response to the end-Cretaceous warm event in the Tropical Pacific. Palaeogeography, Palaeoclimatology, Palaeoecology 291, 239–252.

Van Sickel, W.A., Kominz, M.A., Miller, K.G., Browning, J.V., 2004. Late Cretaceous and Cenozoic sea-level estimates: backstripping analysis of borehole data, onshore New Jersey. Basin Research 16, 451–465.

Veizer, J., Godderis, Y., Francois, L.M., 2000. Evidence for decoupling of atmospheric CO_2 and global climate during the Phanerozoic eon. Nature 408, 698–701.

Wallmann, K., 2001. Controls on the Cretaceous and Cenozoic evolution of seawater composition, atmospheric CO_2 and climate. Geochimica et Cosmochimica Acta 65, 3005–3025.

Wan, X.Q., Chen, P.J., Wei, M.J., 2007. The Cretaceous System in China. Acta Geologica Sinica—English Edition 81, 957–983.

Wang, C.S., Feng, Z.Q., Wu, H.Y., Wang, P.J., Kong, F.J., Feng, Z.H., Ren, Y.G., Yang, G.S., Wan, X.Q., Huang, Y.J., Zhang, S.H., 2008. Preliminary achievement of the Chinese Cretaceous Continental Scientific Drilling Project-SK-I. Acta Geologica Sinica 82, 9–20 (in Chinese, English abstract).

Wang, C.S., Huang, Y.J., Zhao, X.X., 2009. Unlocking a Cretaceous geologic and geophysical puzzle: scientific drilling of Songliao Basin in northeast China. The Leading Edge 28, 340–344.

Westerhold, T., Rohl, U., Donner, B., McCarren, H.K., Zachos, J.C., 2011. A complete high-resolution Paleocene benthic stable isotope record for the central Pacific (ODP Site 1209). Paleoceanography 26, PA2216. http://dx.doi.org/10.1029/2010PA002092.

Wilf, P., Johnson, K.R., Huber, B.T., 2003. Correlated terrestrial and marine evidence for global climate changes before mass extinction at the Cretaceous–Paleogene boundary. Proceedings of the National Academy of Sciences of the United States of America 100, 599–604.

Wolbach, W.S., Gilmour, I., Anders, E., Orth, C.J., Brooks, R.R., 1988. Global fire at the Cretaceous/Tertiary boundary. Nature 334, 665–669.

Wolbach, W.S., Gilmour, I., Anders, E., 1990. Major wildfires at the Cretaceous/Tertiary boundary. In: Sharpton, V.L., Ward, P. (Eds.), Global Catastrophes in Earth History: Geological Society of America Special Paper, 247, pp. 391–400.

Wu, H.C., Zhang, S.H., Jiang, G.Q., Huang, Q.H., 2009. The floating astronomical time scale for the terrestrial Late Cretaceous Qingshankou Formation from the Songliao Basin of Northeast China and its stratigraphic and paleoclimate implications. Earth and Planetary Science Letters 278, 308–323.

Wynn, J.G., 2007. Carbon isotope fractionation during decomposition of organic matter in soils and paleosols: implications for paleoecological interpretations of paleosols. Palaeogeography, Palaeoclimatology, Palaeoecology 251, 437–448.

Zachos, J.C., Arthur, M.A., Dean, W.E., 1989. Geochemical evidence for suppression of pelagic marine productivity at the Cretaceous/Tertiary boundary. Nature 337, 61–64.

Zachos, J., Pagani, M., Sloan, L., Thomas, E., Billups, K., 2001. Trends, rhythms, and aberrations in global climate 65 Ma to present. Science 292, 686–693.

Zeebe, R.E., 2001. Seawater pH and isotopic paleotemperatures of Cretaceous oceans. Palaeogeography, Palaeoclimatology, Palaeoecology 170, 49–57.